Comparative study of electron and positron scattering from benzene (C_6H_6) and hexafluorobenzene (C_6F_6) molecules

C. Makochekanwa, O. Sueoka, and M. Kimura
Graduate School of Science and Engineering, Yamaguchi University, Ube, Yamaguchi 755-8611, Japan
(Received 6 May 2003; published 11 September 2003)

Total cross sections (TCSs) for electron and positron scattering from hexafluorobezene (C_6F_6) molecules have been measured by the linear transmission time-of-flight method and are presented. In addition, new systematic measurements have been also carried out for benzene (C_6H_6)-molecule targets. The impact energies are 0.4–1000 eV and 0.2–1000 eV for electron and positron scattering, respectively. For the case of C_6F_6, two resonance peaks have been observed in C_6F_6 electron TCSs: one at 0.8 eV attributed to the resonant capture of the incident electron into the π^* orbital, with the formation of a transient $C_6F_6^-$ anion, and the broad one in the range above 7 eV showing weak spikes at 14 and 30 eV, of which the 14-eV one has been attributed to another negative-ion resonance formation with decomposition either through the reemission of the electron or through dissociative electron attachment leading to F^-, $C_5F_3^-$, and $C_6F_5^-$ fragmented ions. In contrast, the positron TCSs show no conspicuous strong structure but 2 to 3 weak shoulders overlaid on a broad (6–100)-eV peak arising from a series of electronic excitations, positronium formations, and ionizations. A close comparison with those for C_6H_6 sheds much light on better understanding of the underlying dynamics.

DOI: 10.1103/PhysRevA.68.032707 PACS number(s): 34.80.Bm, 34.80.Dp, 36.10.Dr

I. INTRODUCTION

A comparative study of electron and positron scattering dynamics from atoms and molecules reveals a great deal of information that would otherwise not be easy to derive if the analysis was carried out with only one of these. Knowledge of electron-scattering dynamics and corresponding various cross-section data from fluorocarbon molecules such as CHF_3, C_2F_6, C_3F_8, cyclo-C_4F_8 [1], and chlorine substituted methane [2] have received much attention recent years from many experimentalists and theorists, which have important applications in the plasma processing of thin-film coating and fabrications, and semiconductor etching. Positron scattering from atoms and simple molecules is an area that has been experimentally and theoretically studied for a long time up to now [3]. However, as for positron scattering from polyatomic molecules, only investigations on total cross-section measurements have been presented experimentally just for a small number of molecules, and very little study for elastic and inelastic processes. From the theoretical point of view, only recently have some attempts been reported for a limited number of molecular targets [4,5].

Benzene (C_6H_6) as the simplest aromatic hydrocarbon has invited a great deal of research interest from spectroscopic and dynamical points of view because of its importance in various applications, resulting in a large number of experimental investigations on electron scattering for a wide energy range using various approaches that have been reported over the years on those processes, such as negative-ion (anion) formation, total, elastic, and inelastic including ionization. Only recent and relevant references including theory are given here [6–15]. A number of C_6F_6 electron-scattering studies have also been carried out theoretically and experimentally including the anion-formation experiments of Weik and Illenberger [16], electron attachment experiments of Marawar *et al.* [17], and the theoretical and experimental total cross sections of Jiang, Sun, and Wan [9] and Kasperski, Możejko, and Szmytkowski [10], respectively. However, besides these works of electron scattering cited above, we are not aware of any other systematic and comparative studies carried out for both electron and positron impacts on any benzene-related molecules in a wide energy range.

In this paper, electron-and positron-scattering dynamics from C_6F_6 are investigated experimentally, and total cross sections (TCSs) data for 0.4–1000 eV and 0.2–1000 eV for electron and positron scattering, respectively, are presented in comparison with the data of C_6H_6. The electron and positron TCS data for C_6H_6 presented in this paper were published earlier particularly for the lower-energy region below 10 eV by this group [11,18], but for completeness, we repeated the measurement producing more accurate TCSs for C_6H_6, and hence, provide the whole data here. Special attention is given to examine the fluorination effect due to the substitution of the H atom by the F atom between C_6F_6 and C_6H_6. We also include a discussion of the TCS data in relation to the elastic cross-section data of Cho *et al.* [12].

II. EXPERIMENTAL METHOD

The absolute TCSs for electron and positron scattering from these molecules have been measured using the linear transmission time-of-flight method in an apparatus setup similar to our previous measurements [19], and only the main parts will be highlighted here. See the detailed experimental setup in Ref. [19]. An ~80-μCi ^{22}Na radioactive source produces fast positrons, which are converted to a slow beam using an annealed seven-overlapping-layer mesh tungsten moderator set baked at 2100 °C. The energy width of the positron beam was about 2.2 eV. For electron scattering, the slow electrons are produced as secondary electrons emerging from the moderator surfaces after multiple scattering. The electron beam had an energy spread of about 1.4 eV.

Pressure independence of the TCSs was confirmed by car-

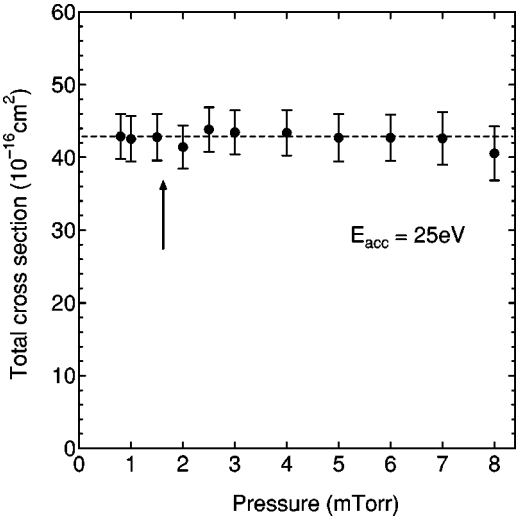

FIG. 1. Electron TCSs for C_6F_6 molecules against collision gas pressure. The beam intensity attenuation (I_v/I_g) of 3 used in our TCS measurements for $E_{acc}=25$ eV is shown by the arrow. Error bars show total uncertainties.

rying out separate experiments at a randomly chosen collision energy value (25 eV) in the current energy range. The results are shown in Fig. 1. As seen in Fig. 1, the TCSs do not show any pressure dependence at all, as has been the case with every other previous study by our group [20].

Total cross-section data

The TCS values Q_t are derived from the Beer-Lambert relation applied as

$$Q_t=(-1/nl)\ln(I_g/I_v), \tag{1}$$

where I_g and I_v refer to the projectile beam intensities transmitted through the collision cell with and without the target gas of number density n, respectively. l refers to the effective length of the collision cell and was established by normalizing our measured positron-N_2 TCSs to those of the positron-N_2 data of Hoffman *et al.* [21]. The purpose of this normalization procedure is not only for the measurement of the effective length, but also for checking the pressure gauge stability. Actually it did not change significantly for each of these measurements.

The numerical data for C_6F_6 electron and positron TCSs are shown in Table I, together with their associated errors determined as follows. The sum of all the uncertainties was estimated to be 5–7.6 % and 6.7–12.3 % for C_6F_6 electron and positron scattering, respectively. This sum of uncertainties is made up of contributions from the $<2.6\%$ for electron and $<7.3\%$ for positron beam intensities, $\Delta I/I$, where I refers to $\ln(I_g/I_v)$ in Eq. (1). The numerical data for C_6H_6 electron and positron TCSs are shown in Table II, together with their associated errors whose sums are estimated to be 4.3–6.5 % and 5.5–10.8 % for electron and positron scattering, respectively. This sum of uncertainties is made up of contributions from $<1.4\%$ for electron and $<5.8\%$ for positron beam intensities, $\Delta I/I$, where I refers to $\ln(I_g/I_v)$ in Eq. (1). The contribution from the gas density was about 3%, while that due to the determination of the effective length of the collision cell, $\Delta l/l$, was about 2% for gases and for both projectiles.

The parallel magnetic field to the flight path, due to the solenoid coils, is applied for beam transportation. The entrance and exit apertures of the collision cell are very wide, being 3 mm in radius. According to these conditions for this apparatus, the measured raw data are fairly affected by forward-scattering effects. The forward-scattering correction was done for both C_6H_6 and C_6F_6, using the method described previously [22]. The correction depends not only on the geometrical conditions including the magnetic field, but also on the differential cross-section (DCS) data. The DCS data used for the forward-scattering correction for these two molecules were the data of Cho *et al.* [12]. The previous data for C_6H_6 [11] were not corrected for the forward-scattering effects. On the other hand, there are no accurate DCS data available for positron scattering in either case and, hence, electron DCS data have been used for correcting the positron TCSs as well.

This correction resulted in increases of the TCS, from the measured value, of 1.5–6 % below 10 eV, 6.5–9 % in the energy range 10–100 eV, and an average 5% above 100 eV, for C_6H_6 electron TCSs. The correction for C_6H_6 positron TCSs resulted in increases of an average 2.5% below 7 eV, about 7–12 % in the energy range 8–100 eV, and an average 7% above 100 eV. The same correction for C_6F_6 also resulted in increases of both electron and positron TCSs as follows. Electron TCSs: about 2.8% below 10 eV, 3.5% at 10–30 eV, 1–3 % at 40–250 eV, and 6.5–19 % at 300–1000 eV for electron TCSs. Positron TCSs: an average 14% below 1.3 eV, about 3.3–7 % at 1.6–40 eV, an average 2% at 50–250 eV, and 9.3–22 % at 300–1000 eV.

III. RESULTS AND DISCUSSION

Both C_6H_6 and C_6F_6 are nonpolar molecules but do have extremely large polarizabilities of 69.4 and 64.6 a.u., respectively, which is surely expected to have a strong influence on low-energy electron scattering. Both molecules have a similar hexagon-shape structure, but the C-H and C-F distances are 1.083 Å and 1.327 Å, respectively [23], and hence, the molecular size of C_6F_6 is larger by roughly 20–30 % than C_6H_6. In addition, electronic structures between these molecules are obviously quite different as the quantum chemistry calculation shows [23] which make scattering events rather distinct from each other particularly below the intermediate-to-low–energy regime. As a general characteristic based on our investigations with many other systems of polyatomic molecules, we have discovered that when hydrogen atoms are replaced by fluorine or chlorine atoms, the resulting increase in molecular size is generally closely linked to an increase in the TCSs for both electron and positron scattering at energy ranges above several hundred eV [4], and this serves as a basis for the additive argument [9], although its validity is very limited and qualitative, but sometimes, questionable. This feature is also observable in the current results as well above 100 eV for both electron and positron as seen

TABLE I. Hexafluorobenzene (C_6F_6) TCSs (10^{-16} cm^2) for electron and positron scattering.

Energy (eV)	Electron	Positron	Energy (eV)	Electron	Positron
0.2		9.9±1.2	11	43.3±2.5	29.0±2.1
0.4	30.7±2.2	13.0±1.2	12	44.7±2.6	31.0±2.3
0.6	33.4±2.2	17.0±1.5	13	45.6±2.7	30.1±2.2
0.8	35.2±2.3	16.3±1.6	14	46.2±2.7	31.0±2.3
1.0	32.9±1.9	17.5±1.3	15	46.7±2.8	30.7±2.2
1.2	31.1±1.9		16	46.5±2.8	29.5±2.2
1.3		18.0±1.3	17	46.6±2.8	30.8±2.3
1.4	28.7±1.8		18	46.7±2.8	31.1±2.4
1.6	27.3±1.8	19.6±1.4	19	46.7±2.8	31.4±2.4
1.8	26.2±1.8		20	46.7±2.8	31.4±2.5
1.9		19.0±1.4	22	47.5±2.7	30.3±2.1
2.0	24.5±1.8		25	47.4±2.9	31.4±2.3
2.2	25.5±1.6	20.7±1.5	30	46.2±3.0	31.3±2.2
2.5	23.6±1.6	20.0±1.5	35	47.4±3.0	
2.8	21.8±1.7	23.0±1.8	40	46.0±2.8	31.2±2.3
3.1	22.3±1.4	21.7±1.7	50	43.1±2.6	30.6±2.4
3.4	21.3±1.4	23.0±1.8	60	41.3±2.5	29.7±2.4
3.7	21.5±1.5	25.5±2.0	70	38.9±2.4	28.6±2.1
4.0	22.3±1.5	25.2±1.8	80	37.6±2.2	29.0±2.0
4.5	25.4±1.6	25.9±1.9	90	35.3±2.1	27.7±1.9
5.0	26.1±1.7	26.2±2.0	100	33.3±2.0	27.0±2.0
5.5	29.8±1.8	25.8±2.0	120	30.7±1.8	26.8±1.9
6	31.3±2.0	26.9±2.0	150	28.7±1.7	24.3±1.8
6.5	33.1±2.0	26.3±2.0	200	25.2±1.4	21.5±1.7
7	33.3±2.1	27.0±2.0	250	23.0±1.3	20.2±1.6
7.5	34.2±2.1	27.0±2.0	300	20.3±1.1	19.6±1.5
8	36.5±2.4	28.2±2.1	400	18.1±1.0	16.7±1.5
8.5	38.4±2.3	28.1±2.1	500	15.6±0.9	13.6±1.4
9	39.2±2.5	29.5±2.2	600	13.9±0.8	13.6±1.1
9.5	40.6±2.5	29.5±2.3	800	11.0±0.6	10.6±0.7
10	41.3±2.4	29.7±2.1	1000	9.5±0.5	8.7±0.7

below. This larger molecular size certainly contributes to greater TCSs than C_6H_6 at 100 eV by 18.8% for electron and 6.3% for positron impacts [see Figs. 3(a) and 3(b) below]. In the low-energy range of a few tens of eV, characteristics in the pattern of TCSs seem to be more dependent on the shape resonances, and the polarization effect is expected to dominate at much lower energies.

We will specifically discuss these features for electron and positron scattering separately in more detail below.

A. Electron TCSs: C_6H_6 and C_6F_6 compared

Figure 2(a) and 2(b) show the results for the present measurements of electron and positron TCSs for C_6F_6 molecules. Also shown in Figs. 2(a) and 2(b) are the results for C_6H_6 molecules for the sake of comparison. Numerical values for C_6F_6 and C_6H_6 TCSs data are given in Tables I and II, respectively, together with their associated errors determined as explained above.

There are some features worth highlighting from the electron TCSs shown in Fig. 2(a). These are summarized as follows.

(i) Both molecules show low-energy resonance peaks, at 0.8 eV for C_6F_6 and 1.6 eV for C_6H_6. The 0.8-eV structure for C_6F_6 has also been observed, together with another one at about 0.4 eV which is not observed in our data, in electron attachment [24–27] as well as in transmission experiments [28]. It has been attributed to the resonant capture of the extra electron into the π^* orbital, with the formation of a transient $C_6F_6^-$ anion. On the other hand, the 1.6-eV structure for C_6H_6 is attributable to electron capture into the degenerate $C_{2u}(\pi^*)$ orbital, yielding the $^2E_{2u}$ electronic state of the $C_6H_6^-$ anion [29], which shows up as a long-lived shape resonance.

(ii) They both have TCSs that decrease below this low-energy peak.

(iii) Both molecules conspicuously show a minimum between 2 and 4 eV, which is shallower for C_6H_6 than C_6F_6.

(iv) An unresolved shoulder is seen at about 4.5 eV in the C_6H_6 TCSs. This can be attributed to the $^2B_{2g}$ resonance observed by Cho *et al.* [12] in their studies where they determined its energy to be 4.94 eV. A resonant structure corresponding to electron capture into the second virtual

TABLE II. Benzene (C_6H_6) TCS (10^{-16} cm^2) for electron and positron scattering.

Energy (eV)	Electron	Positron	Energy (eV)	Electron	Positron
0.2		35.8±3.4	11	59.7±2.8	42.4±2.6
0.4	23.5±1.3	37.8±3.0	12	58.4±2.7	41.1±2.6
0.6	23.5±1.1	41.9±3.0	13	55.3±2.6	41.1±2.7
0.8	24.9±1.4	45.9±3.4	14	53.5±2.5	41.8±2.8
1.0	28.1±1.5	48.5±2.9	15	52.7±2.4	42.5±2.9
1.2	31.6±1.6		16	51.0±2.4	40.8±2.7
1.3		49.6±2.9	17	49.8±2.3	39.9±2.7
1.4	33.4±1.7		18	48.8±2.3	40.4±2.6
1.6	34.2±1.7	50.3±2.9	19	48.8±2.3	39.5±2.6
1.8	33.0±1.6		20	47.7±2.2	37.8±2.6
1.9		50.2±2.9	22	45.7±2.2	37.4±2.3
2.0	32.6±1.7		25	45.5±2.1	37.6±2.6
2.2	32.9±1.6	50.3±2.9	30	44.8±2.1	35.2±2.3
2.5	32.6±1.7	50.5±2.9	35	44.2±2.0	
2.8	34.1±1.8	50.5±3.0	40	42.8±1.9	34.2±2.2
3.1	35.7±1.9	50.5±2.9	50	41.9±1.8	33.1±2.2
3.4	37.0±2.1	50.2±3.0	60	39.3±1.7	31.2±2.1
3.7	39.1±2.3	49.6±2.9	70	36.7±1.6	29.7±2.0
4.0	40.7±2.2	48.4±2.7	80	33.4±1.5	28.4±1.8
4.5	43.1±2.2	48.0±2.7	90	33.3±1.5	28.0±1.8
5.0	45.4±2.2	46.3±2.8	100	30.3±1.3	27.3±1.6
5.5	46.6±2.2	47.0±2.8	120	29.3±1.3	25.1±1.5
6.0	47.6±2.7	46.4±2.9	150	27.1±1.2	23.7±1.7
6.5	48.6±2.3	45.8±2.9	200	24.5±1.1	22.8±1.7
7.0	49.4±2.3	45.8±3.2	250	20.5±0.92	18.9±1.5
7.5	51.7±2.5	45.3±3.0	300	19.1±0.84	16.5±1.2
8.0	54.8±2.5	45.0±3.0	400	14.3±0.65	14.4±1.0
8.5	57.8±2.7	45.1±3.0	500	12.7±0.58	12.9±1.0
9.0	60.0±2.8	45.4±3.1	600	10.4±0.48	10.7±0.7
9.5	59.8±2.8	43.4±2.9	800	7.68±0.37	7.9±0.5
10	59.3±2.9	42.5±2.6	1000	6.15±0.29	6.8±0.5

molecular orbital $1b_{2g}(\pi^*)$ has also been observed at 4.5 eV for C_6F_6 in negative-ion yield curves [16,30] and in the transmission spectra [27]. However, this is not clearly revealed in our TCSs possibly due to low intensity of the resonance process at 4.5 eV, making it difficult to identify it from the sharply increasing TCSs in this region.

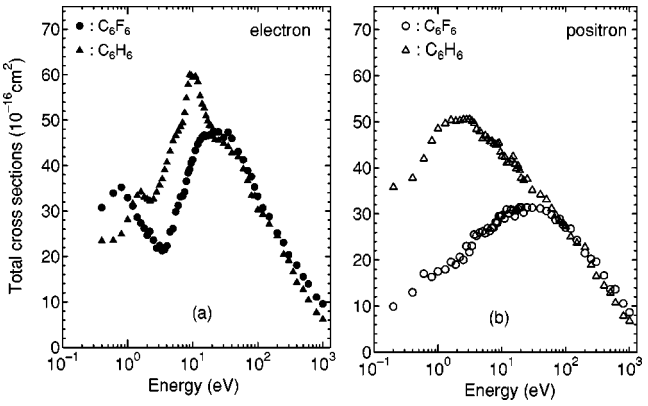

FIG. 2. Electron and positron TCSs for C_6F_6 and C_6H_6 molecules.

(v) Both TCSs rise gradually, above the minimum to produce the prominent peak at 7–13 eV for C_6H_6 and the broad peak composed of two peaks at about 14 and 30 eV for C_6F_6. The (7–13)-eV peak for C_6H_6 is due to a $^2E_{1u}$ shape resonance resulting from the temporal capture of an incident electron into the $\sigma^*(e_{1u})$ orbital, as assigned by Allan [31]. As for C_6F_6, the structure at 14 eV has been attributed to core-excited, temporary, negative-ion resonance formation with decomposition either through the reemission of the incident electron or through dissociative electron attachment (DEA) leading to F^-, $C_5F_3^-$, and $C_6F_5^-$ fragmented ions [10,16].

(vi) At energies above these prominent peak features, both molecules show TCSs that decrease from about 53×10^{-16} cm^2 at 9.5 eV to about 6×10^{-16} cm^2 at 1000 eV for C_6H_6 and from about 52×10^{-16} cm^2 at 30 eV to about 9.5×10^{-16} cm^2 at 1000 eV for C_6F_6.

(vii) C_6F_6 TCSs become greater than C_6H_6 TCSs for all energies above 22 eV.

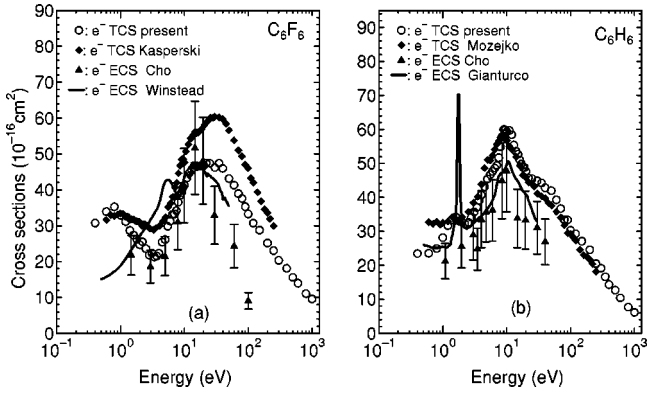

FIG. 3. Electron-scattering TCSs and ECSs for C_6F_6 and C_6H_6 molecules: (a) (○) present C_6F_6 TCS data, (◆) TCS data of Kasperski, Możejko, and Szmytkowski [10], (▲) ECS data of Cho *et al.* [12], and (—) ECS data of Winstead, McKoy, and Bettaga [32]. (b) (○) present C_6H_6 TCS data, (◆) TCS data of Możejko *et al.* [33], (▲) ECS data of Cho *et al.* [12], and (—) ECS data of Gianturco and Lucchese [34].

The effect due to fluorination is manifested itself by several observations: the broadening of the peak for C_6F_6 TCSs (7–80 eV) compared to C_6H_6 TCSs (7–13 eV), the shift in position of the energy of the center of the low-energy peak from 1.6 eV in C_6H_6 to 0.8 eV in C_6F_6, the shift of the main resonance from 8.5 eV in C_6H_6 to about 18 eV for C_6F_6, and larger C_6F_6 TCSs than C_6H_6 TCSs at intermediate to higher energies.

B. Comparison of electron TCSs with other results

Figure 3(a) shows our C_6F_6 TCSs together with those of Kasperski, Możejko, and Szmytkowski [10], the experimental integral elastic cross sections (ECSs) of Cho *et al.* [12], and the theoretical integral ECSs of Winstead, McKoy, and Bettega [32]. Figure 3(b) shows our C_6H_6 TCSs together with those of Możejko *et al.* [33], the experimental integral ECSs of Cho *et al.* [12], and theoretical integral ECSs of Gianturco and Lucchese [34]. As discussed above, DCS results of Cho *et al.* [12], later integrated for the ECSs shown in Fig. 3, were used for the forward-scattering correction of our C_6F_6 and C_6H_6 TCSs shown in Figs. 3(a) and 3(b). Therefore, we take special interest in the comparative study of our TCS with their ECS results.

We discuss the C_6H_6 case first. As in Fig. 3(b), our results are lower than those of Możejko *et al.* [33] below 10 eV, though ours become equal to theirs at about 1.4–1.7 eV where both produce the $^2E_{2u}$ resonance peak. Though discrepancies can be seen between these measurements below 1.5 eV, our data agree fairly well with the recent low-energy data by Gulley *et al.* [15], as qualitatively discussed in our previous paper [18]. Above 10 eV, our TCSs are greater than their measurements over all the energy range they overlap. However, both sets of TCSs generally show the same structures at the same energy locations.

The ECSs of Cho *et al.* [12], with uncertainties estimated to be ±25%, show the same energy dependence with our TCSs. Our TCSs are greater than these ECSs at all energies of overlap; by about 27% at 5 eV, 43% at 20 eV, and 59% at 40 eV. Though the ECS results by Gianturco and Lucchese [34] show the same energy dependence as our TCSs, the 1.6-eV peak in the two experimental TCS measurements, which is only 34.2×10^{-16} cm^2 in magnitude, appears as the sharp spike of about 70×10^{-16} cm^2. The ECSs of Gianturco and Lucchese agree very well with those of Cho *et al.* in the entire energy region they studied. The difference between our TCSs and ECSs represents the sum of all inelastic processes, and the present value in the whole energy region appears reasonably well for representing inelastic contributions, except for the 1.6-eV peak. Rough estimation of the sum from all inelastic processes amounts to 5×10^{-16} cm^2, 12×10^{-16} cm^2, and 16×10^{-16} cm^2 at 3 eV, 10 eV, and 50 eV, respectively. At 3 eV, the dominant contribution to inelastic processes is expected to come from primarily vibrational excitation and, to lesser extent, rotational excitation. At 50 eV, the dominant inelastic process would be ionization, in which we assume that at least 70%, or 11×10^{-16} cm^2, is from that process.

Next we turn to the C_6F_6 case. We assume the C_6F_6 TCS results of Kasperski, Możejko, and Szmytkowski [10] in Fig. 3(a) to have been measured using the same apparatus as the C_6H_6 results of Możejko *et al.* [33], as shown in Fig. 3(b). Therefore, the striking difference in the two TCSs seen between the present and those of Kasperski, Możejko, and Szmytkowski [10] in Fig. 3(a) should be noted, but cannot be easily ascribed to some systematic errors with our apparatus. In general, our TCSs are similar in overall structure to the data of Kasperski, Możejko, and Szmytkowski [10]. Both results show a low-energy resonance peak, at 0.8 eV in the present result while at about 1 eV in the result of Kesperski, Możejko, and Szmytkowski. The minimum at 3 eV, the 14-eV and 30-eV resonance features are also seen in the TCSs of Kasperski, Możejko, and Szmytkowski. However, the behavior of our TCSs around 30 eV is not directly reproduced in their measurements, but rather as a smooth peak. Besides, our TCSs are lower than those of Kasperski, Możejko, and Szmytkowski over all the energy range above 1 eV; being about 25% lower at 3 eV, 12% lower at 6 eV, 20% lower at around 35 eV, and an average 18% lower at energies over the range of overlap above 70 eV. From our systematic comparison for all molecules so far we have studied and our good agreement with their results up to mid 1990s, we tend to believe that the experimental results after late 1990s by the Gdansk group are consistently larger due, probably, to a problem in their pressure gauge.

The general features and shape between our TCSs and ECSs of Cho *et al.* are in good accord in the whole energy region studied. Specifically the general structure of our TCSs is reproduced in ECSs' of Cho *et al.*; the rising trend at low energies below 3 eV, followed by the minimum at about 3 eV, the rising trend in the region of 3.5–10 eV, and the fall-off trend at higher energies. The resonance structure at 14 eV is well reproduced except that the ECSs become greater than TCSs between 12 and 18 eV in absolute value, though the ±25% error in their data would remove the inconsistency. The structure at 30 eV is not reproduced in the ECS results suggesting that it should possibly be from ionization, elec-

tronic excitation, and a possible DEA. The ECSs of Winstead, McKoy, and Bettega [32] is not consistent with our TCSs as well as ECSs of Cho *et al.* both in energy dependence and magnitude in the entire energy region they studied. It appears that if we shift their results by 10 eV to higher-energy side, then some agreement can be forced to achieve. For example, their peak at 5 eV may correspond to ours at 14 eV, and a second larger hump in the neighborhood of 10–25 eV to that of ours at 20–50 eV. It misses the minimum at 3.5 eV, but seems to reach its own minimum below 0.5 eV. Again, the difference between the present TCSs and ECSs of Cho *et al.* gives the sum of all inelastic processes for electron scattering from C_6F_6. Rough estimate suggests that 3×10^{-16} cm^2, 4×10^{-16} cm^2, and 16×10^{-16} cm^2 at 5 eV, 10 eV, and 30 eV, respectively. These difference values are smaller than those of C_6H_6 particularly for smaller energy domain below 10 eV, suggesting smaller contributions from vibrational excitation for C_6F_6 because of heavier fluorine atoms.

C. Positron TCSs: C_6H_6 and C_6F_6 compared

Figure 2(b) shows the positron TCSs for C_6F_6 and C_6H_6 molecules. As far as we know there are no other positron-scattering TCS measurements done with these molecules. Just as for the electron case, although ionization, elastic, various excitation, and other partial cross-section measurements are needed for full elucidation of the features that are observed in our positron TCSs, some interesting features seen in this figure are highlighted here.

(i) Both molecules show broad peaks, which are about 0.6–20 eV for C_6H_6 and 6–100 eV for C_6F_6 molecules. These peaks are centered at 2 eV for C_6H_6 and 25 eV for C_6F_6 molecules.

(ii) TCSs decrease on either side of this peak for both molecules. However in the lower-energy region, the decrease below the peak is fairly rapid for C_6H_6 TCSs as compared to C_6F_6. This phenomenon of the rapid decrease in C_6H_6 positron TCSs below 1 eV has been qualitatively studied [18] and is tentatively attributed to the near-zero scattering for positron impact causing the sharp drop because of the delicate balance between the attractive and repulsive interactions at these energies.

(iii) C_6H_6 TCSs are greater than those of C_6F_6 at energies below 60 eV even though C_6F_6 is larger in size than C_6H_6. This characteristic is similar to the electron-scattering case. The reason for this could be due partially to a larger polarization interaction effect in the C_6H_6 than in the C_6F_6 system.

(iv) Above the peak, both TCSs decrease with basically the same slope.

(v) Both TCSs merge becoming nearly the same magnitude above ~100 eV.

As mentioned earlier, several small structures and shoulders can be seen in both TCSs in the energy from ~3.5 to 20 eV or so, arising from positronium formation, a series of electronic excitations and ionizations, although these structures are much weaker than those seen in electron counterparts. That C_6F_6 TCSs show a peak at a position shifted to higher energies compared to C_6H_6 TCSs and that the peak is broader than that for C_6H_6 TCSs can be viewed as some results of the fluorination effect in positron scattering.

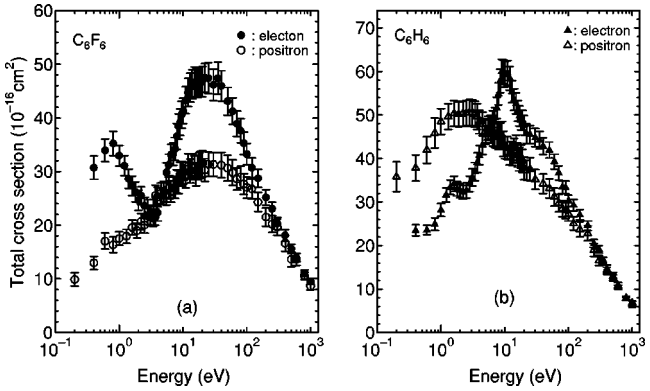

FIG. 4. Electron and positron TCSs for C_6F_6 and C_6H_6 molecules.

D. Comparison of electron and positron TCSs

Figures 4(a) and 4(b) show the electron and positron TCSs drawn separately for these two molecules. One striking feature immediately seen in the figures would be that, below 5 eV, positron TCSs become greater than electron TCSs in the case of C_6H_6, whereas there is no such crossover is observed in C_6F_6 TCSs. This turn-around feature between electron and positron TCSs below a few eV domain has been studied carefully earlier for electron and positron impacts on CO_2 molecule and other simpler molecules systematically by us, and we tentatively concluded that rotational excitation for positron impact becomes more efficient than electron counterparts for some cases where they have negative quadrupole interactions [35,36]. Alternatively, there may be a case where vibrational excitation for positron impact is more effective resulting in a larger TCS, or positron attachment may be also a possible cause for a larger TCS. More careful and comprehensive theoretical investigations to elucidate this point further are certainly needed.

From C_6F_6 in Fig. 4(a) it can be observed in that, below 3 eV, electron TCSs rise to produce the 0.8-eV resonance peak before decreasing rapidly at energies below this peak, against continuously decreasing positron TCSs. Electron TCSs show a minimum at 3.5 eV before rising, with increasing energy, rather sharply to produce the broad resonance peaks described above, between 14 and 35 eV. Positron TCSs, on the other hand, show a gradual increase, with weak but not negligible structures as described in the preceding section, to produce the broad peak centered at around 25 eV. Electron TCSs are greater than positron TCSs in any energy region studied, being more than one and a half times greater between 15 and 40 eV. This has been the case observed with most of the polyatomic molecules studied in our laboratory, and has been explained by a combination of stronger interactions and the presence of resonances in electron than positron scattering in this energy region. Both TCSs decrease above 70 eV and become nearly equal above a few hundred eV.

From C_6H_6 in Fig. 4(b), electron TCSs are smaller by a factor of 1.7 nearly in all energies than those of positron below about 5 eV, but are larger above this energy. Two TCSs begin to merge above 100 eV. As discussed above, we have observed in a few molecular cases that positron TCSs become larger than electron counterparts in the energy region between 2–3 eV and −0.5 eV, but normally the difference between electron and positron TCSs would be of the order of a few tens of percents. In this C_6H_6 case, the difference is much larger, probably, due to the fact that a large number of rovibrational excitation modes effectively participate in making far larger positron TCSs. In addition, positron attachment may also take place nearby negatively charged carbon atoms forming a cage structure, which may be more efficient than being trapped outside, contrary to electron attachment to positively charged hydrogen atoms in the outer region of the molecule. Theoretical investigation of positron attachment to various hydrocarbons is now underway by using rigorous quantum chemistry configuration-interaction method, and the results will be reported in a separate paper [37].

IV. CONCLUSION

In this paper, TCS measurements for (0.4–1000)-eV electron and (0.2–1000)-eV positron scattering from hexafluorobenzene (C_6F_6) molecules have been presented, and a comparative study with C_6H_6 measured results was carried out. Two resonance peaks have been observed in C_6F_6 electron TCSs at 0.8 eV, attributed to the resonant capture with the formation of a transient $C_6F_6^-$ anion, and at 7–80 eV showing weak structures at 14 and 30 eV with decomposition either through the reemission of the incident electron or through DEA leading to F^-, $C_5F_3^-$, and $C_6F_5^-$ fragmented ions. In contrast, the positron TCSs show no conspicuous structure but a broad peak in the neighborhood of 6–100 eV.

The comparison between C_6F_6 and C_6H_6 showed C_6H_6 electron TCSs becoming greater than C_6F_6 TCSs between 1.7 and 13 eV. This should be resulting from the enhancement due to the overlapping of the $^2E_{2u}$ shape resonance between 1 and 2 eV, the $^2B_{2g}$ resonance at 4.9 eV, and the $^2E_{1u}$ shape resonance in the region of 8.5 eV combined in this region. The positron TCSs showed the striking behavior of C_6H_6 TCSs becoming increasingly greater at low energies than those of C_6F_6 which is large in size. Both electron and positron TCSs decrease above 30 eV with C_6F_6 TCSs being greater than C_6H_6 TCSs. The broadening of the peak for C_6F_6 TCSs (7–80 eV) compared to C_6H_6 TCSs (7–13 eV), the shift in position of the energy of the center of the peak to higher energies for C_6F_6, and the fact that at intermediate to higher energies C_6F_6 TCSs become greater than C_6H_6 TCSs are attributed to the fluorination effect in electron scattering. For positron scattering, this effect has been viewed as responsible for the shift of the peak position to a higher energy for C_6F_6 TCSs compared to C_6H_6 TCSs, and for the broader C_6F_6 TCSs peak (6–100 eV) than that for C_6H_6 TCSs (0.4–20 eV).

ACKNOWLEDGMENTS

This work was supported in part by a Grant-in-Aid from the Ministry of Education, Science, Technology, Sport and Culture, Japan Society for Promotion of Science (JSPS), and a Cooperative Research Grant from the National Institute for Fusion Science, Japan.

[1] J. E. Sanabia, G. D. Cooper, J. A. Tossel, and J. H. Moore, J. Chem. Phys. **108**, 389 (1998).
[2] G. P. Karwasz, R. S. Brusa, A. Piazza, and A. Zecca, Phys. Rev. A **59**, 1341 (1999).
[3] M. Chaltron, Rep. Prog. Phys. **48**, 737 (1985).
[4] M. Kimura, O. Sueoka, A. Hamada, and Y. Itikawa, Adv. Chem. Phys. **111**, 537 (1999).
[5] O. Sueoka, M. K. Kawada, and M. Kimura, Nucl. Instrum. Methods Phys. Res. B **171**, 96 (2000).
[6] R. J. Gulley and S. J. Buckman, J. Phys. B **32**, L405 (1999).
[7] S. Leach, J. Electron Spectrosc. Relat. Phenom. **41**, 427 (1986).
[8] P. D. Burrow, J. A. Michejda, and K. D. Jordan, J. Chem. Phys. **86**, 9 (1987).
[9] Y. Jiang, J. Sun, and L. Wan, Phys. Rev. A **62**, 062712 (2000).
[10] G. Kasperski, P. Możejko, and C. Szmytkowski, Z. Phys. D: At., Mol. Clusters **42**, 187 (1997).
[11] O. Sueoka, J. Phys. B **21**, L631 (1988).
[12] H. Cho, R. J. Gulley, K. Sunohara, M. Kitajima, L. J. Uhlmann, H. Tanaka, and S. J. Buckman, J. Phys. B **34**, 1019 (2001).
[13] R. Azria and G. Schulz, J. Chem. Phys. **62**, 573 (1975).
[14] D. Mathur and J. B. Hasted, J. Phys. B **9**, L31 (1976).
[15] R. J. Gulley, S. L. Lunt, J.-P. Ziesel, and D. Field, J. Phys. B **31**, 2735 (1998).
[16] F. Weik and E. Illenberger, J. Chem. Phys. **103**, 1406 (1995).
[17] R. W. Marawar, C. W. Walter, K. A. Smith, and F. B. Dunning, J. Chem. Phys. **88**, 2853 (1988).
[18] M. Kimura, C. Makochekanwa, and O. Sueoka, Phys. Rev. A (to be published).
[19] O. Sueoka and S. Mori, J. Phys. B **19**, 4035 (1986).
[20] O. Sueoka, C. Makochekanwa, and H. Kawate, Nucl. Instrum. Methods Phys. Res. B **192**, 206 (2002).
[21] K. R. Hoffman, M. S. Dababneh, Y.-F. Hsieh, W. E. Kauppila, V. Pol, J. H. Smart, and T. S. Stein, Phys. Rev. A **25**, 1393 (1982).
[22] A. Hamada and O. Sueoka, J. Phys. B **27**, 5055 (1994).
[23] J. Almlof and K. Faegril, Jr., J. Chem. Phys. **79**, 2284 (1983).
[24] P. G. Datskos, L. G. Christophorou, and J. G. Canter, J. Chem. Phys. **98**, 7875 (1993).
[25] K. S. Gant and L. G. Christophorou, J. Chem. Phys. **65**, 2977 (1976).
[26] H. Shimamori, T. Sunagawa, Y. Ogawa, and Y. Tatsumi, Chem. Phys. Lett. **227**, 609 (1994).
[27] L. G. Christophorou and P. G. Datskos, Int. J. Mass Spectrom. Ion Processes **149/150**, 59 (1995).

[28] J. R. Frazier, L. G. Christophorou, and J. G. Canter, J. Chem. Phys. **69**, 3807 (1978).
[29] L. Sanche and G. J. Schulz, J. Chem. Phys. **58**, 479 (1973).
[30] M. Fenzlaff and E. Illenberger, Chem. Phys. **136**, 443 (1989).
[31] M. Allan, J. Electron Spectrosc. Relat. Phenom. **48**, 219 (1989).
[32] C. Winstead, V. McKoy, and M. H. F. Bettega, Bull. Am. Phys. Soc. **44** (1999).
[33] P. Możejko, G. Kasperski, C. Szmytkowski, G. P. Karwasz, R. S. Brussa, and A. Zecca, Chem. Phys. Lett. **257**, 309 (1996).
[34] F. A. Gianturco and R. R. Lucchese, J. Chem. Phys. **108**, 6144 (1998).
[35] K. Takayanagi and M. Inokuti, J. Phys. Soc. Jpn. **21**, 837 (1967).
[36] M. Kimura, O. Sueoka, A. Hamada, M. Takekawa, Y. Itikawa, H. Tanaka, and L. Boesten, J. Chem. Phys. **107**, 6616 (1997).
[37] M. Tachikawa, R. J. Buenker, and M. Kimura, J. Chem. Phys. (to be published).